Study of multilayered composites through periodic homogenization and Mori-Tanaka methods

George Chatzigeorgiou

Study of multilayered composites through periodic homogenization and Mori-Tanaka methods

George Chatzigeorgiou

Arts et Metiers Institute of Technology, CNRS, Université de Lorraine, LEM3-UMR 7239, F-57070 Metz, France

Abstract

The multilayered composite structure has been utilized frequently in the literature of periodic homogenization as a test case for developing new methodologies for linear and nonlinear composite media. The manuscript demonstrates that these composites can also be used for validating mean-field micromechanics techniques. It is shown the the Mori-Tanaka method combined with the Transformation Field Analysis provides the same solution with the periodic homogenization for nonlinear multilayered composites.

Keywords: multilayered composites; periodic homogenization; Mori-Tanaka method; Transformation Field Analysis; inelastic fields.

1. Introduction

Composite materials are complicated media whose microstructure contains two or more different material phases. Their study is performed using the so-called multiscale modeling approaches, which rely on the concept of scale separation. According to these methods, the behavior of the overall

Email address: georges.chatzigeorgiou@ensam.eu (George Chatzigeorgiou)

structure is identified through splitting it into several scales. Specially designed average techniques allow to study at first the finer scales and identify "homogenized properties" that pass to the next (higher) scale.

The mechanical behavior of highly heterogeneous, nonlinear composite materials has been the subject of many researchers in the last 30 years. Several multiscale methods have been developed for identifying the overall response of viscoelastic, elastoplastic, viscoplastic, or damaged composite materials (Suquet, 1987; Ponte-Castañeda, 1991; Terada and Kikuchi, 2001; Desrumaux et al., 2001; Meraghni et al., 2002; Yu and Fish, 2002; Aboudi et al., 2003; Aboudi, 2004; Chaboche et al., 2005; Love and Batra, 2006; Asada and Ohno, 2007; Jendli et al., 2009; Mercier and Molinari, 2009; Khatam and Pindera, 2010; Cavalcante et al., 2009; Kruch and Chaboche, 2011; Brenner and Suquet, 2013; Tu and Pindera, 2014; Cavalcante and Pindera, 2016; Tikarrouchine et al., 2018; Praud et al., 2021). Review papers discussing the existing techniques have been written by Pindera et al. (2009); Charalambakis (2010); Mercier et al. (2012); Charalambakis et al. (2018).

The periodic homogenization approach, applicable for composite media with periodic microstructure, has been theoretically established by Bensoussan et al. (1978); Sanchez-Palencia (1978); Murat and Tartar (1997), and nowadays it is considered classical and among the most accurate homogenization theories. This method has been also adopted for inelastic, periodic heterogeneous media (Suquet, 1987; Fish et al., 1997; Herzog and Jacquet, 2007). Recent developments of the theory permit to account for gradient phenomena, complex nonlinear responses and multiphysics mechanisms. The most common example for validating the classical periodic homogenization and

its extensions is the study of mutilayered periodic composites (Kalamkarov and Kolpakov, 1997; Fish and Chen, 2001; Yu and Fish, 2002; Otero et al., 2005; Chatzigeorgiou et al., 2015, 2016). The advantage of these heterogeneous media is that all the equations at the unit cell level are reduced to one dimensional (in terms of spatial coordinates), transforming the equilibrium from partial differential to ordinary differential equations problem. Such simplification permits to obtain analytical or semi-analytical solution for the macroscopic properties and fields. The periodically multilayered structure, to the best of the author's knowledge, is not examined in the mean-field micromechanics community.

The scope of the current manuscript is to demonstrate that mean-field approaches can also predict the response of the multilayered composites. It is shown that the Mori-Tanaka method (Mori and Tanaka, 1973; Benveniste, 1987; Buryachenko, 2007; Dvorak, 2013), combined with the Transformation Field Analysis (TFA) approach (Dvorak and Benveniste, 1992), provides the same solution with the periodic homogenization independently of the anisotropic level of the layers.

The structure of the manuscript is as follows: Several mathematical formulas, helpful for the study of the unit cell problem (or representative volume element, in case of the mean-field method), are given in section 2. Section 3 presents the unit cell solution of the multilayered medium, according to the periodic homogenization theory. The Mori-Tanaka/TFA approach for the same composite is presented in section 4. A numerical example, illustrating the efficiency of the mean-field technique, is provided in section 5 and the main text finishes with the conclusions of the work. The Hill polarization

tensor for a disk-like inclusion in an infinite anisotropic medium is given in an appendix at the end of the article.

2. Mathematical preliminaries

In the computations of the multilayered composite's unit cell, it is useful to write the normal and tangential parts (with respect to the axis x_1) of the second order tensors separately. For a strain tensor $\boldsymbol{\varepsilon}$, and a stress tensor $\boldsymbol{\sigma}$, written in Voigt notation[1] as

$$\boldsymbol{\varepsilon} = \begin{bmatrix} \varepsilon_{11} \\ \varepsilon_{22} \\ \varepsilon_{33} \\ 2\varepsilon_{12} \\ 2\varepsilon_{13} \\ 2\varepsilon_{23} \end{bmatrix}, \qquad \boldsymbol{\sigma} = \begin{bmatrix} \sigma_{11} \\ \sigma_{22} \\ \sigma_{33} \\ \sigma_{12} \\ \sigma_{13} \\ \sigma_{23} \end{bmatrix}, \tag{1}$$

respectively, the normal and tangential parts are expressed through the 3×1 vectors

$$\begin{aligned} \boldsymbol{\varepsilon}_n &= \begin{bmatrix} \varepsilon_{11} \\ 2\varepsilon_{12} \\ 2\varepsilon_{13} \end{bmatrix}, \qquad \boldsymbol{\varepsilon}_t = \begin{bmatrix} \varepsilon_{22} \\ \varepsilon_{33} \\ 2\varepsilon_{23} \end{bmatrix}, \\ \boldsymbol{\sigma}_n &= \begin{bmatrix} \sigma_{11} \\ \sigma_{12} \\ \sigma_{13} \end{bmatrix}, \qquad \boldsymbol{\sigma}_t = \begin{bmatrix} \sigma_{22} \\ \sigma_{33} \\ \sigma_{23} \end{bmatrix}. \end{aligned} \tag{2}$$

[1]The Voigt notation presented here considers as fourth element the shear term 12 and as sixth element the shear term 23. This small deviation from the classical Voigt representation does not alter the results.

A fourth order tensor $\boldsymbol{D}$ that presents minor symmetries ($D_{ijkl} = D_{jikl} = D_{ijlk}$) is written in the Voigt form

$$\boldsymbol{D} = \begin{bmatrix} D_{11} & D_{12} & D_{13} & D_{14} & D_{15} & D_{16} \\ D_{21} & D_{22} & D_{23} & D_{24} & D_{25} & D_{26} \\ D_{31} & D_{32} & D_{33} & D_{34} & D_{35} & D_{36} \\ D_{41} & D_{42} & D_{43} & D_{44} & D_{45} & D_{46} \\ D_{51} & D_{52} & D_{53} & D_{54} & D_{55} & D_{56} \\ D_{61} & D_{62} & D_{63} & D_{64} & D_{65} & D_{66} \end{bmatrix}. \tag{3}$$

This tensor can be represented with the help of the following four matrices:

$$\boldsymbol{D}_{nn} = \begin{bmatrix} D_{11} & D_{14} & D_{15} \\ D_{41} & D_{44} & D_{45} \\ D_{51} & D_{54} & D_{55} \end{bmatrix}, \quad \boldsymbol{D}_{nt} = \begin{bmatrix} D_{12} & D_{13} & D_{16} \\ D_{42} & D_{43} & D_{46} \\ D_{52} & D_{53} & D_{56} \end{bmatrix},$$
$$\boldsymbol{D}_{tn} = \begin{bmatrix} D_{21} & D_{24} & D_{25} \\ D_{31} & D_{34} & D_{35} \\ D_{61} & D_{64} & D_{65} \end{bmatrix}, \quad \boldsymbol{D}_{tt} = \begin{bmatrix} D_{22} & D_{23} & D_{26} \\ D_{32} & D_{33} & D_{36} \\ D_{62} & D_{63} & D_{66} \end{bmatrix}, \tag{4}$$

through the matrix-type expression

$$\boldsymbol{D} = \boldsymbol{\mathcal{I}}_n \cdot \boldsymbol{D}_{nn} \cdot \boldsymbol{\mathcal{I}}_n^T + \boldsymbol{\mathcal{I}}_n \cdot \boldsymbol{D}_{nt} \cdot \boldsymbol{\mathcal{I}}_t^T + \boldsymbol{\mathcal{I}}_t \cdot \boldsymbol{D}_{tn} \cdot \boldsymbol{\mathcal{I}}_n^T + \boldsymbol{\mathcal{I}}_t \cdot \boldsymbol{D}_{tt} \cdot \boldsymbol{\mathcal{I}}_t^T, \tag{5}$$

in which the superscipt T denotes the usual transpose operation, while the 6×3 matrices $\boldsymbol{\mathcal{I}}_n$ and $\boldsymbol{\mathcal{I}}_t$ are given by

$$\boldsymbol{\mathcal{I}}_n = \begin{bmatrix} 1 & 0 & 0 \\ 0 & 0 & 0 \\ 0 & 0 & 0 \\ 0 & 1 & 0 \\ 0 & 0 & 1 \\ 0 & 0 & 0 \end{bmatrix}, \qquad \boldsymbol{\mathcal{I}}_t = \begin{bmatrix} 0 & 0 & 0 \\ 1 & 0 & 0 \\ 0 & 1 & 0 \\ 0 & 0 & 0 \\ 0 & 0 & 0 \\ 0 & 0 & 1 \end{bmatrix}. \tag{6}$$

Let's assume that the tensor $\boldsymbol{D}$ connects two symmetric second order tensors $\boldsymbol{a}$ and $\boldsymbol{b}$ (strain or stress type). The relation in indicial (Einstein's) notation

$$a_{ij} = D_{ijkl} b_{kl},$$

can be represented, using the normal and tangential parts, in the matrix forms

$$\boldsymbol{a}_n = \boldsymbol{D}_{nn} \cdot \boldsymbol{b}_n + \boldsymbol{D}_{nt} \cdot \boldsymbol{b}_t, \qquad \boldsymbol{a}_t = \boldsymbol{D}_{tn} \cdot \boldsymbol{b}_n + \boldsymbol{D}_{tt} \cdot \boldsymbol{b}_t.$$

When $\boldsymbol{D}$ possesses major symmetries ($D_{ijkl} = D_{klij}$), then

$$\boldsymbol{D}_{nn} = \boldsymbol{D}_{nn}^T, \quad \boldsymbol{D}_{tn} = \boldsymbol{D}_{nt}^T, \quad \boldsymbol{D}_{tt} = \boldsymbol{D}_{tt}^T.$$

Important properties of the matrices $\boldsymbol{\mathcal{I}}_n$ and $\boldsymbol{\mathcal{I}}_t$ are the following:

$$\boldsymbol{\mathcal{I}}_n \cdot \boldsymbol{I} \cdot \boldsymbol{\mathcal{I}}_n^T + \boldsymbol{\mathcal{I}}_t \cdot \boldsymbol{I} \cdot \boldsymbol{\mathcal{I}}_t^T = \boldsymbol{\mathcal{I}},$$

where

$$\boldsymbol{\mathcal{I}} = \begin{bmatrix} 1 & 0 & 0 & 0 & 0 & 0 \\ 0 & 1 & 0 & 0 & 0 & 0 \\ 0 & 0 & 1 & 0 & 0 & 0 \\ 0 & 0 & 0 & 1 & 0 & 0 \\ 0 & 0 & 0 & 0 & 1 & 0 \\ 0 & 0 & 0 & 0 & 0 & 1 \end{bmatrix}, \quad \boldsymbol{I} = \begin{bmatrix} 1 & 0 & 0 \\ 0 & 1 & 0 \\ 0 & 0 & 1 \end{bmatrix},$$

$$\boldsymbol{\mathcal{I}}_n^T \cdot \boldsymbol{\varepsilon} = \boldsymbol{\varepsilon}_n, \qquad \boldsymbol{\mathcal{I}}_t^T \cdot \boldsymbol{\varepsilon} = \boldsymbol{\varepsilon}_t,$$
$$\boldsymbol{\mathcal{I}}_n^T \cdot \boldsymbol{\mathcal{I}}_t = \boldsymbol{\mathcal{I}}_t^T \cdot \boldsymbol{\mathcal{I}}_n = \boldsymbol{0}, \qquad \boldsymbol{\mathcal{I}}_n^T \cdot \boldsymbol{\mathcal{I}}_n = \boldsymbol{\mathcal{I}}_t^T \cdot \boldsymbol{\mathcal{I}}_t = \boldsymbol{I}.$$

The general stress-strain relation of an inelastic material is expressed in indicial (Einstein's) notation as

$$\sigma_{ij} = L_{ijkl}\varepsilon_{kl} + \sigma_{ij}^p, \tag{7}$$

where L_{ijkl} is the elasticity tensor (fourth order with minor and major symmetries) and σ_{ij}^p denotes the inelastic part of the stress. When the material experiences damage mechanism, the tensor L_{ijkl} depends on the damage state. The discussed framework in this work can accomodate damage conditions. In such cases, L_{ijkl} is referred to as secant modulus.

Equation (7) can be expressed in terms on normal and tangential parts (with respect to the axis x_1) in the matrix forms

$$\begin{aligned} \boldsymbol{\sigma}_n &= \boldsymbol{L}_{nn} \cdot \boldsymbol{\varepsilon}_n + \boldsymbol{L}_{nt} \cdot \boldsymbol{\varepsilon}_t + \boldsymbol{\sigma}_n^p, \\ \boldsymbol{\sigma}_t &= \boldsymbol{L}_{nt}^T \cdot \boldsymbol{\varepsilon}_n + \boldsymbol{L}_{tt} \cdot \boldsymbol{\varepsilon}_t + \boldsymbol{\sigma}_t^p. \end{aligned} \tag{8}$$

3. Periodic homogenization for multilayered composite structures

As already mentioned in the introduction, the periodic homogenization framework is well established in the literature. When dealing with nonlinear composites, incremental/iterational schemes are required. It is usually more convenient for FE computations to utilize a tangential type of approach (Terada and Kikuchi, 2001; Asada and Ohno, 2007; Chatzigeorgiou et al., 2016, 2018), in which the elasticity tensor is substituted by the state-dependent tangent modulus. Here, for comparison reasons with the Mori-Tanaka/Transformation Field Analysis method, the stress is represented by the general relation (7).

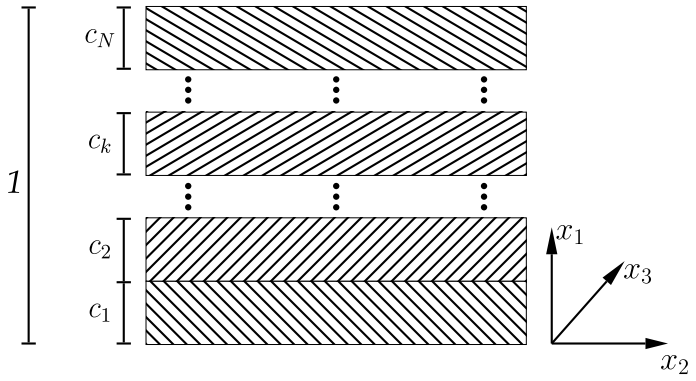

Figure 1: Unit cell of multilayered composite with N layers.

Let's consider a multilayered composite structure, whose unit cell is shown in Figure 1. This unit cell consists of N distinct, possibly anisotropic, layers, each one having its own volume fraction (c_k for the k_{th} layer).

The stress in an arbitrary r_{th} layer of the unit cell is given by

$$\sigma_{ij}^{(r)} = L_{ijkl}^{(r)} \varepsilon_{kl}^{(r)} + \sigma_{ij}^{p(r)}, \qquad r \geqslant 1, \quad \forall x \in \left(\sum_{q=0}^{r-1} c_q, \sum_{q=0}^{r} c_q \right). \tag{9}$$

Fo convenience in the above and the following expressions, c_0 is considered equal to 0. According to the periodic homogenization theory of first order, the microscopic displacement and strain at the r_{th} layer can be written as

$$\begin{aligned} u_i^{(r)} &= \bar{\varepsilon}_{ij} x_j + \widetilde{u}_i^{(r)}, \\ \varepsilon_{ij}^{(r)} &= \bar{\varepsilon}_{ij}^{(r)} + \frac{1}{2}\frac{\partial \widetilde{u}_i^{(r)}}{\partial x_j} + \frac{1}{2}\frac{\partial \widetilde{u}_j^{(r)}}{\partial x_i}, \\ r \geqslant 1, \qquad & \forall x \in \left(\sum_{q=0}^{r-1} c_q, \sum_{q=0}^{r} c_q \right). \end{aligned} \tag{10}$$

$\bar{\boldsymbol{\varepsilon}}$ corresponds to the macroscopic total strain. In the sequel, a bar above a symbol will denote a macroscopic quantity. The displacement field $\widetilde{\boldsymbol{u}}$ is periodic.

The equilibrium equations per layer, as well as the traction and displacement continuity conditions between the layers read

$$\begin{aligned} &\frac{\partial \sigma_{ij}^{(r)}}{\partial x_j} = 0, \qquad r \geqslant 1, \quad \forall x \in \left(\sum_{q=0}^{r-1} c_q, \sum_{q=0}^{r} c_q \right), \\ &\sigma_{i1}^{(r-1)} = \sigma_{i1}^{(r)} \qquad \text{at} \quad x = \sum_{q=1}^{r-1} c_q, \quad r \geqslant 2, \\ &\widetilde{u}_i^{(r-1)} = \widetilde{u}_i^{(r)} \qquad \text{at} \quad x = \sum_{q=1}^{r-1} c_q, \quad r \geqslant 2. \end{aligned} \tag{11}$$

In the multilayered unit cell, derivatives with respect to x_2 and x_3 vanish. For simplification in the computations, the vector and matrix representations of section 2 are introduced. Since only the derivatives with respect to x_1

remain, one obtains

$$\begin{aligned} \boldsymbol{\varepsilon}_n^{(r)} &= \bar{\boldsymbol{\varepsilon}}_n + \frac{\mathrm{d}\widetilde{\boldsymbol{u}}^{(r)}}{\mathrm{d}x_1}, \qquad \widetilde{\boldsymbol{u}}^{(r)} = \begin{bmatrix} \widetilde{u}_1^{(r)} \\ \widetilde{u}_2^{(r)} \\ \widetilde{u}_3^{(r)} \end{bmatrix}, \\ \boldsymbol{\varepsilon}_t^{(r)} &= \bar{\boldsymbol{\varepsilon}}_t, \end{aligned} \tag{12}$$

for the strains and

$$\begin{aligned} \boldsymbol{\sigma}_n^{(r)} &= \boldsymbol{L}_{nn}^{(r)} \cdot \left[\bar{\boldsymbol{\varepsilon}}_n + \frac{\mathrm{d}\widetilde{\boldsymbol{u}}^{(r)}}{\mathrm{d}x_1} \right] + \boldsymbol{L}_{nt}^{(r)} \cdot \bar{\boldsymbol{\varepsilon}}_t + \boldsymbol{\sigma}_n^{p(r)}, \\ \boldsymbol{\sigma}_t^{(r)} &= \left[\boldsymbol{L}_{nt}^{(r)} \right]^T \cdot \left[\bar{\boldsymbol{\varepsilon}}_n + \frac{\mathrm{d}\widetilde{\boldsymbol{u}}^{(r)}}{\mathrm{d}x_1} \right] + \boldsymbol{L}_{tt}^{(r)} \cdot \bar{\boldsymbol{\varepsilon}}_t + \boldsymbol{\sigma}_t^{p(r)}. \end{aligned} \tag{13}$$

for the stresses. Moreover, the equilibrium per layer is written

$$\frac{\mathrm{d}\boldsymbol{\sigma}_n^{(r)}}{\mathrm{d}x_1} = \boldsymbol{0} \quad \Rightarrow \quad \boldsymbol{\sigma}_n^{(r)} = \bar{\boldsymbol{\sigma}}_n. \tag{14}$$

The last relation indicates that the normal stress part, $\boldsymbol{\sigma}_n^{(r)}$, of any layer is equal to its macroscopic counterpart $\bar{\boldsymbol{\sigma}}_n$. From the equilibrium, the derivative of $\widetilde{\boldsymbol{u}}$ is obtained as

$$\frac{\mathrm{d}\widetilde{\boldsymbol{u}}^{(r)}}{\mathrm{d}x_1} = \left[\boldsymbol{L}_{nn}^{(r)} \right]^{-1} \cdot \bar{\boldsymbol{\sigma}}_n - \widehat{\boldsymbol{\varepsilon}}_n^{(r)}, \tag{15}$$

where

$$\widehat{\boldsymbol{\varepsilon}}_n^{(r)} = \bar{\boldsymbol{\varepsilon}}_n + \left[\boldsymbol{L}_{nn}^{(r)} \right]^{-1} \cdot \left[\boldsymbol{\sigma}_n^{p(r)} + \boldsymbol{L}_{nt}^{(r)} \cdot \bar{\boldsymbol{\varepsilon}}_t \right]. \tag{16}$$

Integrating with respect to x_1 yields

$$\widetilde{\boldsymbol{u}}^{(r)}(x_1) = \left[\left[\boldsymbol{L}_{nn}^{(r)} \right]^{-1} \cdot \bar{\boldsymbol{\sigma}}_n - \widehat{\boldsymbol{\varepsilon}}_n^{(r)} \right] x_1 + \boldsymbol{\omega}^{(r)}, \tag{17}$$

where $\boldsymbol{\omega}^{(r)}$ are constant vectors. The periodicity conditions on the displacement fields give

$$\widetilde{\boldsymbol{u}}^{(1)}(0) = \widetilde{\boldsymbol{u}}^{(N)}(1) \quad \Rightarrow \quad \boldsymbol{\omega}^{(1)} - \boldsymbol{\omega}^{(N)} = \left[\boldsymbol{L}_{nn}^{(N)}\right]^{-1} \cdot \overline{\boldsymbol{\sigma}}_n - \widehat{\boldsymbol{\varepsilon}}_n^{(N)}. \tag{18}$$

The displacement continuity at the interfaces yields the relations

$$\left[\left[\boldsymbol{L}_{nn}^{(1)}\right]^{-1} \cdot \overline{\boldsymbol{\sigma}}_n - \widehat{\boldsymbol{\varepsilon}}_n^{(1)}\right] c_1 + \boldsymbol{\omega}^{(1)} = \left[\left[\boldsymbol{L}_{nn}^{(2)}\right]^{-1} \cdot \overline{\boldsymbol{\sigma}}_n - \widehat{\boldsymbol{\varepsilon}}_n^{(2)}\right] c_1 + \boldsymbol{\omega}^{(2)},$$

$$\left[\left[\boldsymbol{L}_{nn}^{(2)}\right]^{-1} \cdot \overline{\boldsymbol{\sigma}}_n - \widehat{\boldsymbol{\varepsilon}}_n^{(2)}\right] \sum_{q=1}^{2} c_q + \boldsymbol{\omega}^{(2)} = \left[\left[\boldsymbol{L}_{nn}^{(3)}\right]^{-1} \cdot \overline{\boldsymbol{\sigma}}_n - \widehat{\boldsymbol{\varepsilon}}_n^{(3)}\right] \sum_{q=1}^{2} c_q + \boldsymbol{\omega}^{(3)},$$

$$\vdots$$

$$\left[\left[\boldsymbol{L}_{nn}^{(k)}\right]^{-1} \cdot \overline{\boldsymbol{\sigma}}_n - \widehat{\boldsymbol{\varepsilon}}_n^{(k)}\right] \sum_{q=1}^{k} c_q + \boldsymbol{\omega}^{(k)} =$$
$$\left[\left[\boldsymbol{L}_{nn}^{(k+1)}\right]^{-1} \cdot \overline{\boldsymbol{\sigma}}_n - \widehat{\boldsymbol{\varepsilon}}_n^{(k+1)}\right] \sum_{q=1}^{k} c_q + \boldsymbol{\omega}^{(k+1)},$$

$$\vdots$$

$$\left[\left[\boldsymbol{L}_{nn}^{(N-1)}\right]^{-1} \cdot \overline{\boldsymbol{\sigma}}_n - \widehat{\boldsymbol{\varepsilon}}_n^{(N-1)}\right] \sum_{q=1}^{N-1} c_q + \boldsymbol{\omega}^{(N-1)} =$$
$$\left[\left[\boldsymbol{L}_{nn}^{(N)}\right]^{-1} \cdot \overline{\boldsymbol{\sigma}}_n - \widehat{\boldsymbol{\varepsilon}}_n^{(N)}\right] \sum_{q=1}^{N-1} c_q + \boldsymbol{\omega}^{(N)}.$$

Adding all the above expressions and taking into account the boundary condition (18) leads to the expression

$$\sum_{r=1}^{N} c_r \left[\left[\boldsymbol{L}_{nn}^{(r)}\right]^{-1} \cdot \overline{\boldsymbol{\sigma}}_n - \widehat{\boldsymbol{\varepsilon}}_n^{(r)}\right] = \boldsymbol{0},$$

or

$$\bar{\boldsymbol{\sigma}}_n = \boldsymbol{M}_{nn} \cdot \bar{\boldsymbol{\varepsilon}}_n + \boldsymbol{M}_{nn} \cdot \boldsymbol{M}_{nt} \cdot \bar{\boldsymbol{\varepsilon}}_t + \boldsymbol{M}_{nn} \cdot \boldsymbol{m}_n^p, \tag{19}$$

with

$$\begin{aligned} \boldsymbol{M}_{nn} &= \left[\sum_{r=1}^{N} c_r \left[\boldsymbol{L}_{nn}^{(r)} \right]^{-1} \right]^{-1}, \\ \boldsymbol{M}_{nt} &= \sum_{r=1}^{N} c_r \left[\boldsymbol{L}_{nn}^{(r)} \right]^{-1} \boldsymbol{L}_{nt}^{(r)}, \\ \boldsymbol{m}_n^p &= \sum_{r=1}^{N} c_r \left[\boldsymbol{L}_{nn}^{(r)} \right]^{-1} \boldsymbol{\sigma}_n^{p(r)}. \end{aligned} \tag{20}$$

Returning to equations (12) one has

$$\begin{aligned} \boldsymbol{\varepsilon}_n^{(r)} &= \left[\boldsymbol{L}_{nn}^{(r)} \right]^{-1} \cdot \boldsymbol{M}_{nn} \cdot \bar{\boldsymbol{\varepsilon}}_n + \left[\boldsymbol{L}_{nn}^{(r)} \right]^{-1} \cdot \left[\boldsymbol{M}_{nn} \cdot \boldsymbol{M}_{nt} - \boldsymbol{L}_{nt}^{(r)} \right] \cdot \bar{\boldsymbol{\varepsilon}}_t \\ &\quad + \left[\boldsymbol{L}_{nn}^{(r)} \right]^{-1} \cdot \left[\boldsymbol{M}_{nn} \cdot \boldsymbol{m}_n^p - \boldsymbol{\sigma}_n^{p(r)} \right], \\ \boldsymbol{\varepsilon}_t^{(r)} &= \bar{\boldsymbol{\varepsilon}}_t. \end{aligned} \tag{21}$$

Algebraic manipulations give

$$\begin{aligned} \boldsymbol{\varepsilon}_n^{(r)} &= \left[\boldsymbol{L}_{nn}^{(r)} \right]^{-1} \cdot \boldsymbol{M}_{nn} \cdot \bar{\boldsymbol{\varepsilon}}_n + \left[\boldsymbol{L}_{nn}^{(r)} \right]^{-1} \cdot \boldsymbol{M}_{nn} \cdot \left[\boldsymbol{M}_{nt} - \boldsymbol{M}_{nn}^{-1} \cdot \boldsymbol{L}_{nt}^{(r)} \right] \cdot \bar{\boldsymbol{\varepsilon}}_t \\ &\quad + \left[\boldsymbol{L}_{nn}^{(r)} \right]^{-1} \cdot \boldsymbol{M}_{nn} \cdot \left[\boldsymbol{m}_n^p - \boldsymbol{M}_{nn}^{-1} \cdot \boldsymbol{\sigma}_n^{p(r)} \right], \end{aligned}$$

or, in summary,

$$
\begin{aligned}
\boldsymbol{\varepsilon}_n^{(r)} &= \boldsymbol{A}_{nn}^{(r)} \cdot \bar{\boldsymbol{\varepsilon}}_n + \boldsymbol{A}_{nt}^{(r)} \cdot \bar{\boldsymbol{\varepsilon}}_t + \sum_{q=1}^{N} c_q \boldsymbol{A}_{nn}^{p(qr)} \cdot \left[\boldsymbol{\sigma}_n^{p(q)} - \boldsymbol{\sigma}_n^{p(r)} \right], \\
\boldsymbol{\varepsilon}_t^{(r)} &= \bar{\boldsymbol{\varepsilon}}_t, \\
\boldsymbol{A}_{nn}^{(r)} &= \left[\boldsymbol{L}_{nn}^{(r)} \right]^{-1} \cdot \left[\sum_{q=1}^{N} c_q \left[\boldsymbol{L}_{nn}^{(q)} \right]^{-1} \right]^{-1}, \\
\boldsymbol{A}_{nt}^{(r)} &= \boldsymbol{A}_{nn}^{(r)} \cdot \sum_{q=1}^{N} c_q \left[\boldsymbol{L}_{nn}^{(q)} \right]^{-1} \left[\boldsymbol{L}_{nt}^{(q)} - \boldsymbol{L}_{nt}^{(r)} \right], \\
\boldsymbol{A}_{nn}^{p(qr)} &= \boldsymbol{A}_{nn}^{(r)} \cdot \left[\boldsymbol{L}_{nn}^{(q)} \right]^{-1}.
\end{aligned} \tag{22}
$$

Equations (22) state that the strain fields (and consequently the stress fields) take different values at the various layers, but they remain uniform inside a single layer. $\boldsymbol{A}^{(r)}$ correspond to the well-known strain concentration tensors.

4. Mori-Tanaka/TFA method for multilayered composites

Homogenization techniques based on the Eshelby problems (for instance Mori-Tanaka or self consistent), have been proven to be very efficient for elastic composites (Mura, 1987; Benveniste, 1987; Qu and Cherkaoui, 2006). However, when nonlinear components are present, these methods usually lead to stiff response and certain modifications are required (Doghri and Ouaar, 2003; Chaboche et al., 2005; Lahellec and Suquet, 2007; Brassart et al., 2012; Barral et al., 2020; Chen et al., 2021). This is due to the underlying hypothesis that each material phase is described by a single set of internal variables (for instance inelastic strains or damage). Such assumption is not valid in the majority of the composite materials where a matrix phase is present. In the multilayered composites though, the assumption is valid. According to the

unit cell solution provided by periodic homogenization illustrates (see previous section), the mechanical fields are uniform inside a single layer, which also means that the response of a layer is described by a single set of internal variables.

The Mori-Tanaka method is very popular among the existing micromechanics methods, but has certain limitations. Its most important problem is related to the loss of symmetry of the elasticity tensor when mutiple types of heterogeneities (i.e. different types of ellipsoids) appear in the composite (Benveniste et al., 1991). More advanced micromechanics techniques, like the Ponte-Castañeda and Willis (1995) or the Effective Field Method (Buryachenko, 2007), may provide better overall response estimate. In the composite examined here, where only one type of aligned inclusions is considered, both the Ponte-Castañeda and Willis approach and the Effective Field Method lead to the same macroscopic response as the Mori-Tanaka.

To apply the Mori-Tanaka approach, the presence of a reference material in the representative volume element is required. In particulate or fiber reinforced media, the reference material is the matrix phase. In multilayered composites the notion of reference material is arbitrary, thus any one of the unit cell layers can play this role. In this work the layer 1 is chosen to represent the "matrix" phase.

In the mean-field, Eshelby based methodologies, two fourth order tensors are introduced: the Hill polarization tensor and the dilute strain concentration tensor.

The Hill polarization tensor, $\boldsymbol{P}$, for a disk-like inclusion (x_1 dimension much much smaller than the other two) embedded in a medium with elasticity

tensor $\boldsymbol{L}^{(1)}$ is given by

$$\boldsymbol{P} = \boldsymbol{I}_1 \cdot \left[\boldsymbol{L}_{nn}^{(1)}\right]^{-1} \cdot \boldsymbol{I}_1^T. \tag{23}$$

The proof of this expression is given in the appendix A.

The dilute strain concentration tensor, $\boldsymbol{T}^{(r)}$, is an important operator that connects the strains between the r_{th} phase and the reference material. The inverse of $\boldsymbol{T}^{(r)}$ is given in indicial notation by

$$\left[T_{ijkl}^{(r)}\right]^{-1} = \mathcal{I}_{ijkl} + P_{ijmn}\left[L_{mnkl}^{(r)} - L_{mnkl}^{(1)}\right]. \tag{24}$$

In matrix notation this gives

$$\begin{aligned}
\left[\boldsymbol{T}^{(r)}\right]^{-1} &= \boldsymbol{\mathcal{I}} + \boldsymbol{P} \cdot \left[\boldsymbol{L}^{(r)} - \boldsymbol{L}^{(1)}\right] \\
&= \boldsymbol{\mathcal{I}}_n \cdot \boldsymbol{I} \cdot \boldsymbol{\mathcal{I}}_n^T + \boldsymbol{\mathcal{I}}_t \cdot \boldsymbol{I} \cdot \boldsymbol{\mathcal{I}}_t^T \\
&\quad + \boldsymbol{\mathcal{I}}_n \cdot \left[\boldsymbol{L}_{nn}^{(1)}\right]^{-1} \cdot \left[\boldsymbol{L}_{nn}^{(r)} - \boldsymbol{L}_{nn}^{(1)}\right] \cdot \boldsymbol{\mathcal{I}}_n^T \\
&\quad + \boldsymbol{\mathcal{I}}_n \cdot \left[\boldsymbol{L}_{nn}^{(1)}\right]^{-1} \cdot \left[\boldsymbol{L}_{nt}^{(r)} - \boldsymbol{L}_{nt}^{(1)}\right] \cdot \boldsymbol{\mathcal{I}}_t^T \\
&= \boldsymbol{\mathcal{I}}_n \cdot \left[\boldsymbol{L}_{nn}^{(1)}\right]^{-1} \cdot \boldsymbol{L}_{nn}^{(r)} \cdot \boldsymbol{\mathcal{I}}_n^T + \boldsymbol{\mathcal{I}}_t \cdot \boldsymbol{I} \cdot \boldsymbol{\mathcal{I}}_t^T \\
&\quad + \boldsymbol{\mathcal{I}}_n \cdot \left[\boldsymbol{L}_{nn}^{(1)}\right]^{-1} \cdot \left[\boldsymbol{L}_{nt}^{(r)} - \boldsymbol{L}_{nt}^{(1)}\right] \cdot \boldsymbol{\mathcal{I}}_t^T.
\end{aligned} \tag{25}$$

Let's assume that the dilute strain concentration tensor has similar form, i.e.

$$\boldsymbol{T}^{(r)} = \boldsymbol{\mathcal{I}}_n \cdot \boldsymbol{K}_1 \cdot \boldsymbol{\mathcal{I}}_n^T + \boldsymbol{\mathcal{I}}_n \cdot \boldsymbol{K}_2 \cdot \boldsymbol{\mathcal{I}}_t^T + \boldsymbol{\mathcal{I}}_t \cdot \boldsymbol{K}_3 \cdot \boldsymbol{\mathcal{I}}_t^T. \tag{26}$$

where $\boldsymbol{K}_1$, $\boldsymbol{K}_2$ and $\boldsymbol{K}_3$ are 3×3 matrices. Due to the uniqueness of $\boldsymbol{T}^{(r)}$, if the hypothesis is correct, then the computations will provide a unique solution for the tensor. From the relation $\boldsymbol{\mathcal{I}} = \left[\boldsymbol{T}^{(r)}\right]^{-1} \cdot \boldsymbol{T}^{(r)}$ one has

$$\begin{aligned}
&\boldsymbol{\mathcal{I}}_n \cdot \boldsymbol{I} \cdot \boldsymbol{\mathcal{I}}_n^T + \boldsymbol{\mathcal{I}}_t \cdot \boldsymbol{I} \cdot \boldsymbol{\mathcal{I}}_t^T = \boldsymbol{\mathcal{I}}_n \cdot \left[\boldsymbol{L}_{nn}^{(1)}\right]^{-1} \cdot \boldsymbol{L}_{nn}^{(r)} \cdot \boldsymbol{K}_1 \cdot \boldsymbol{\mathcal{I}}_n^T + \boldsymbol{\mathcal{I}}_t \cdot \boldsymbol{K}_3 \cdot \boldsymbol{\mathcal{I}}_t^T \\
&\quad + \boldsymbol{\mathcal{I}}_n \cdot \left[\left[\boldsymbol{L}_{nn}^{(1)}\right]^{-1} \cdot \boldsymbol{L}_{nn}^{(r)} \cdot \boldsymbol{K}_2 + \left[\boldsymbol{L}_{nn}^{(1)}\right]^{-1} \cdot \left[\boldsymbol{L}_{nt}^{(r)} - \boldsymbol{L}_{nt}^{(1)}\right] \cdot \boldsymbol{K}_3\right] \cdot \boldsymbol{\mathcal{I}}_t^T,
\end{aligned} \tag{27}$$

which leads to the three equations

$$\begin{aligned}
\boldsymbol{I} &= \left[\boldsymbol{L}_{nn}^{(1)}\right]^{-1} \cdot \boldsymbol{L}_{nn}^{(r)} \cdot \boldsymbol{K}_1, \\
\boldsymbol{I} &= \boldsymbol{K}_3, \\
\boldsymbol{0} &= \left[\boldsymbol{L}_{nn}^{(1)}\right]^{-1} \cdot \boldsymbol{L}_{nn}^{(r)} \cdot \boldsymbol{K}_2 + \left[\boldsymbol{L}_{nn}^{(1)}\right]^{-1} \cdot \left[\boldsymbol{L}_{nt}^{(r)} - \boldsymbol{L}_{nt}^{(1)}\right] \cdot \boldsymbol{K}_3.
\end{aligned} \tag{28}$$

These equations provide the unique solution

$$\begin{aligned}
\boldsymbol{K}_1 &= \left[\boldsymbol{L}_{nn}^{(r)}\right]^{-1} \cdot \boldsymbol{L}_{nn}^{(1)}, \\
\boldsymbol{K}_3 &= \boldsymbol{I}, \\
\boldsymbol{K}_2 &= -\left[\boldsymbol{L}_{nn}^{(r)}\right]^{-1} \cdot \left[\boldsymbol{L}_{nt}^{(r)} - \boldsymbol{L}_{nt}^{(1)}\right].
\end{aligned} \tag{29}$$

Thus, the dilute strain concentration tensor is expressed as

$$\begin{aligned}
\boldsymbol{T}^{(r)} &= \boldsymbol{\mathcal{I}}_n \cdot \left[\boldsymbol{L}_{nn}^{(r)}\right]^{-1} \cdot \boldsymbol{L}_{nn}^{(1)} \cdot \boldsymbol{\mathcal{I}}_n^T + \boldsymbol{\mathcal{I}}_t \cdot \boldsymbol{I} \cdot \boldsymbol{\mathcal{I}}_t^T \\
&\quad -\boldsymbol{\mathcal{I}}_n \cdot \left[\boldsymbol{L}_{nn}^{(r)}\right]^{-1} \cdot \left[\boldsymbol{L}_{nt}^{(r)} - \boldsymbol{L}_{nt}^{(1)}\right] \cdot \boldsymbol{\mathcal{I}}_t^T.
\end{aligned} \tag{30}$$

According to the Mori-Tanaka approach, the strain on the r_{th} phase and the strain in the infinite medium, when both are subjected to uniform inelastic stresses, are connected through the formulas (Dvorak and Benveniste, 1992)

$$\varepsilon_{ij}^{(r)} = T_{ijkl}^{(r)} \varepsilon_{kl}^{(1)} + T_{ijmn}^{(r)} P_{mnkl} \left[\sigma_{kl}^{p(1)} - \sigma_{kl}^{p(r)}\right]. \tag{31}$$

Using the matrix representation and the formulas (23) and (30) yields

$$\begin{aligned}
\boldsymbol{\varepsilon}^{(r)} &= \boldsymbol{\mathcal{I}}_n \cdot \left[\boldsymbol{L}_{nn}^{(r)}\right]^{-1} \cdot \boldsymbol{L}_{nn}^{(1)} \cdot \boldsymbol{\varepsilon}_n^{(1)} + \boldsymbol{\mathcal{I}}_t \cdot \boldsymbol{\varepsilon}_t^{(1)} \\
&\quad -\boldsymbol{\mathcal{I}}_n \cdot \left[\boldsymbol{L}_{nn}^{(r)}\right]^{-1} \cdot \left[\boldsymbol{L}_{nt}^{(r)} - \boldsymbol{L}_{nt}^{(1)}\right] \cdot \boldsymbol{\varepsilon}_t^{(1)} \\
&\quad +\boldsymbol{\mathcal{I}}_n \cdot \left[\boldsymbol{L}_{nn}^{(r)}\right]^{-1} \cdot \left[\boldsymbol{\sigma}_n^{p(1)} - \boldsymbol{\sigma}_n^{p(r)}\right].
\end{aligned} \tag{32}$$

Thus,

$$\begin{aligned}
\boldsymbol{\varepsilon}_n^{(r)} &= \boldsymbol{\mathcal{I}}_n^T \cdot \boldsymbol{\varepsilon}^{(r)} = \left[\boldsymbol{L}_{nn}^{(r)}\right]^{-1} \cdot \boldsymbol{L}_{nn}^{(1)} \cdot \boldsymbol{\varepsilon}_n^{(1)} \\
&\quad - \left[\boldsymbol{L}_{nn}^{(r)}\right]^{-1} \cdot \left[\boldsymbol{L}_{nt}^{(r)} - \boldsymbol{L}_{nt}^{(1)}\right] \cdot \boldsymbol{\varepsilon}_t^{(1)} \\
&\quad + \left[\boldsymbol{L}_{nn}^{(r)}\right]^{-1} \cdot \left[\boldsymbol{\sigma}_n^{p(1)} - \boldsymbol{\sigma}_n^{p(r)}\right], \\
\boldsymbol{\varepsilon}_t^{(r)} &= \boldsymbol{\mathcal{I}}_t^T \cdot \boldsymbol{\varepsilon}^{(r)} = \boldsymbol{\varepsilon}_t^{(1)}.
\end{aligned} \tag{33}$$

The macroscopic strain can be expressed as

$$\begin{aligned}
\bar{\boldsymbol{\varepsilon}}_n &= \sum_{q=1}^{N} c_q \boldsymbol{\varepsilon}_n^{(q)} = \sum_{q=1}^{N} c_q \left[\boldsymbol{L}_{nn}^{(q)}\right]^{-1} \cdot \boldsymbol{L}_{nn}^{(1)} \cdot \boldsymbol{\varepsilon}_n^{(1)} \\
&\quad - \sum_{q=1}^{N} c_q \left[\boldsymbol{L}_{nn}^{(q)}\right]^{-1} \cdot \left[\boldsymbol{L}_{nt}^{(q)} - \boldsymbol{L}_{nt}^{(1)}\right] \cdot \boldsymbol{\varepsilon}_t^{(1)} \\
&\quad + \sum_{q=1}^{N} c_q \left[\boldsymbol{L}_{nn}^{(q)}\right]^{-1} \cdot \left[\boldsymbol{\sigma}_n^{p(1)} - \boldsymbol{\sigma}_n^{p(q)}\right], \\
\bar{\boldsymbol{\varepsilon}}_t &= \sum_{q=1}^{N} c_q \boldsymbol{\varepsilon}_t^{(q)} = \boldsymbol{\varepsilon}_t^{(1)}.
\end{aligned} \tag{34}$$

In the above relation it has been used that

$$\begin{aligned}
c_1 \boldsymbol{\varepsilon}_n^{(1)} &= c_1 \left[\boldsymbol{L}_{nn}^{(1)}\right]^{-1} \cdot \boldsymbol{L}_{nn}^{(1)} \cdot \boldsymbol{\varepsilon}_n^{(1)} \\
&\quad + c_1 \left[\boldsymbol{L}_{nn}^{(1)}\right]^{-1} \cdot \left[\boldsymbol{L}_{nt}^{(1)} - \boldsymbol{L}_{nt}^{(1)}\right] \cdot \boldsymbol{\varepsilon}_t^{(1)} \\
&\quad + c_1 \left[\boldsymbol{L}_{nn}^{(1)}\right]^{-1} \cdot \left[\boldsymbol{\sigma}_n^{p(1)} - \boldsymbol{\sigma}_n^{p(1)}\right].
\end{aligned} \tag{35}$$

As a conclusion of (34), one has

$$\begin{aligned}
\boldsymbol{\varepsilon}_n^{(1)} &= \boldsymbol{A}_{nn}^{(1)} \cdot \bar{\boldsymbol{\varepsilon}}_n + \boldsymbol{A}_{nt}^{(1)} \cdot \bar{\boldsymbol{\varepsilon}}_t + \sum_{q=1}^{N} c_q \boldsymbol{A}_{nn}^{p(q1)} \cdot \left[\boldsymbol{\sigma}_n^{p(q)} - \boldsymbol{\sigma}_n^{p(1)}\right], \\
\boldsymbol{\varepsilon}_t^{(1)} &= \bar{\boldsymbol{\varepsilon}}_t,
\end{aligned} \tag{36}$$

where

$$\begin{aligned}
\boldsymbol{A}_{nn}^{(1)} &= \left[\boldsymbol{L}_{nn}^{(1)}\right]^{-1} \cdot \left[\sum_{q=1}^{N} c_q \left[\boldsymbol{L}_{nn}^{(q)}\right]^{-1}\right]^{-1}, \\
\boldsymbol{A}_{nt}^{(1)} &= \boldsymbol{A}_{nn}^{(1)} \cdot \sum_{q=1}^{N} c_q \left[\boldsymbol{L}_{nn}^{(q)}\right]^{-1} \left[\boldsymbol{L}_{nt}^{(q)} - \boldsymbol{L}_{nt}^{(1)}\right], \\
\boldsymbol{A}_{nn}^{p(q1)} &= \boldsymbol{A}_{nn}^{(1)} \cdot \left[\boldsymbol{L}_{nn}^{(q)}\right]^{-1}. \qquad (37)
\end{aligned}$$

Returning back to (33) yields

$$\begin{aligned}
\boldsymbol{\varepsilon}_n^{(r)} &= \boldsymbol{A}_{nn}^{(r)} \cdot \bar{\boldsymbol{\varepsilon}}_n + \boldsymbol{A}_{nt}^{(r)} \cdot \bar{\boldsymbol{\varepsilon}}_t + \boldsymbol{K}, \\
\boldsymbol{\varepsilon}_t^{(r)} &= \bar{\boldsymbol{\varepsilon}}_t, \qquad (38)
\end{aligned}$$

with

$$\begin{aligned}
\boldsymbol{A}_{nn}^{(r)} &= \left[\boldsymbol{L}_{nn}^{(r)}\right]^{-1} \cdot \boldsymbol{L}_{nn}^{(1)} \cdot \boldsymbol{A}_{nn}^{(1)} \\
&= \left[\boldsymbol{L}_{nn}^{(r)}\right]^{-1} \cdot \left[\sum_{q=1}^{N} c_q \left[\boldsymbol{L}_{nn}^{(q)}\right]^{-1}\right]^{-1},
\end{aligned}$$

$$\begin{aligned}
\boldsymbol{A}_{nt}^{(r)} &= \left[\boldsymbol{L}_{nn}^{(r)}\right]^{-1} \cdot \boldsymbol{L}_{nn}^{(1)} \cdot \boldsymbol{A}_{nt}^{(1)} - \left[\boldsymbol{L}_{nn}^{(r)}\right]^{-1} \cdot \left[\boldsymbol{L}_{nt}^{(r)} - \boldsymbol{L}_{nt}^{(1)}\right] \\
&= \boldsymbol{A}_{nn}^{(r)} \cdot \sum_{q=1}^{N} c_q \left[\boldsymbol{L}_{nn}^{(q)}\right]^{-1} \left[\boldsymbol{L}_{nt}^{(q)} - \boldsymbol{L}_{nt}^{(1)}\right] \\
&\quad - \boldsymbol{A}_{nn}^{(r)} \cdot \sum_{q=1}^{N} c_q \left[\boldsymbol{L}_{nn}^{(q)}\right]^{-1} \left[\boldsymbol{L}_{nt}^{(r)} - \boldsymbol{L}_{nt}^{(1)}\right] \\
&= \boldsymbol{A}_{nn}^{(r)} \cdot \sum_{q=1}^{N} c_q \left[\boldsymbol{L}_{nn}^{(q)}\right]^{-1} \left[\boldsymbol{L}_{nt}^{(q)} - \boldsymbol{L}_{nt}^{(r)}\right],
\end{aligned}$$

$$
\begin{aligned}
\boldsymbol{K} &= \left[\boldsymbol{L}_{nn}^{(r)}\right]^{-1} \cdot \boldsymbol{L}_{nn}^{(1)} \cdot \boldsymbol{A}_{nn}^{(1)} \cdot \sum_{q=1}^{N} c_q \left[\boldsymbol{L}_{nn}^{(q)}\right]^{-1} \cdot \left[\boldsymbol{\sigma}_n^{p(q)} - \boldsymbol{\sigma}_n^{p(1)}\right] \\
&\quad + \left[\boldsymbol{L}_{nn}^{(r)}\right]^{-1} \cdot \left[\boldsymbol{\sigma}_n^{p(1)} - \boldsymbol{\sigma}_n^{p(r)}\right] \\
&= \boldsymbol{A}_{nn}^{(r)} \cdot \sum_{q=1}^{N} c_q \left[\boldsymbol{L}_{nn}^{(q)}\right]^{-1} \cdot \left[\boldsymbol{\sigma}_n^{p(q)} - \boldsymbol{\sigma}_n^{p(1)}\right] \\
&\quad + \boldsymbol{A}_{nn}^{(r)} \cdot \sum_{q=1}^{N} c_q \left[\boldsymbol{L}_{nn}^{(q)}\right]^{-1} \cdot \left[\boldsymbol{\sigma}_n^{p(1)} - \boldsymbol{\sigma}_n^{p(r)}\right] \\
&= \boldsymbol{A}_{nn}^{(r)} \cdot \sum_{q=1}^{N} c_q \left[\boldsymbol{L}_{nn}^{(q)}\right]^{-1} \cdot \left[\boldsymbol{\sigma}_n^{p(q)} - \boldsymbol{\sigma}_n^{p(r)}\right].
\end{aligned}
$$

To summarize, for all layers the obtained relations are

$$
\begin{aligned}
\boldsymbol{\varepsilon}_n^{(r)} &= \boldsymbol{A}_{nn}^{(r)} \cdot \bar{\boldsymbol{\varepsilon}}_n + \boldsymbol{A}_{nt}^{(r)} \cdot \bar{\boldsymbol{\varepsilon}}_t + \sum_{q=1}^{N} c_q \boldsymbol{A}_{nn}^{p(qr)} \cdot \left[\boldsymbol{\sigma}_n^{p(q)} - \boldsymbol{\sigma}_n^{p(r)}\right], \\
\boldsymbol{\varepsilon}_t^{(r)} &= \bar{\boldsymbol{\varepsilon}}_t, \\
\boldsymbol{A}_{nn}^{(r)} &= \left[\boldsymbol{L}_{nn}^{(r)}\right]^{-1} \cdot \left[\sum_{q=1}^{N} c_q \left[\boldsymbol{L}_{nn}^{(q)}\right]^{-1}\right]^{-1}, \\
\boldsymbol{A}_{nt}^{(r)} &= \boldsymbol{A}_{nn}^{(r)} \cdot \sum_{q=1}^{N} c_q \left[\boldsymbol{L}_{nn}^{(q)}\right]^{-1} \left[\boldsymbol{L}_{nt}^{(q)} - \boldsymbol{L}_{nt}^{(r)}\right], \\
\boldsymbol{A}_{nn}^{p(qr)} &= \boldsymbol{A}_{nn}^{(r)} \cdot \left[\boldsymbol{L}_{nn}^{(q)}\right]^{-1}.
\end{aligned} \tag{39}
$$

The formulas (39) and (22) are identical.

The rest of the microscopic and macroscopic fields for both the periodic homogenization and the Mori-Tanaka mean-field method are derived in a similar manner. The microscopic stress at each layer is given by the expression

(9) or (8):

$$
\begin{aligned}
\boldsymbol{\sigma}_n^{(r)} &= \boldsymbol{L}_{nn}^{(r)} \cdot \boldsymbol{\varepsilon}_n^{(r)} + \boldsymbol{L}_{nt}^{(r)} \cdot \boldsymbol{\varepsilon}_t^{(r)} + \boldsymbol{\sigma}_n^{p(r)} \\
&= \boldsymbol{L}_{nn}^{(r)} \cdot \boldsymbol{A}_{nn}^{(r)} \cdot \bar{\boldsymbol{\varepsilon}}_n + \left[\boldsymbol{L}_{nn}^{(r)} \cdot \boldsymbol{A}_{nt}^{(r)} + \boldsymbol{L}_{nt}^{(r)} \right] \cdot \bar{\boldsymbol{\varepsilon}}_t \\
&\quad + \sum_{q=1}^{N} c_q \boldsymbol{L}_{nn}^{(r)} \cdot \boldsymbol{A}_{nn}^{p(qr)} \cdot \left[\boldsymbol{\sigma}_n^{p(q)} - \boldsymbol{\sigma}_n^{p(r)} \right] + \boldsymbol{\sigma}_n^{p(r)}, \\
\boldsymbol{\sigma}_t^{(r)} &= \left[\boldsymbol{L}_{nt}^{(r)} \right]^T \cdot \boldsymbol{\varepsilon}_n^{(r)} + \boldsymbol{L}_{tt}^{(r)} \cdot \boldsymbol{\varepsilon}_t^{(r)} + \boldsymbol{\sigma}_t^{p(r)} \\
&= \left[\boldsymbol{L}_{nt}^{(r)} \right]^T \cdot \boldsymbol{A}_{nn}^{(r)} \cdot \bar{\boldsymbol{\varepsilon}}_n + \left[\left[\boldsymbol{L}_{nt}^{(r)} \right]^T \cdot \boldsymbol{A}_{nt}^{(r)} + \boldsymbol{L}_{tt}^{(r)} \right] \cdot \bar{\boldsymbol{\varepsilon}}_t \\
&\quad + \sum_{q=1}^{N} c_q \left[\boldsymbol{L}_{nt}^{(r)} \right]^T \cdot \boldsymbol{A}_{nn}^{p(qr)} \cdot \left[\boldsymbol{\sigma}_n^{p(q)} - \boldsymbol{\sigma}_n^{p(r)} \right] + \boldsymbol{\sigma}_t^{p(r)}.
\end{aligned} \tag{40}
$$

The macroscopic stress is obtained by volume averaging the stresses of all layers, i.e.

$$
\bar{\boldsymbol{\sigma}}_n = \sum_{r=1}^{N} c_r \boldsymbol{\sigma}_n^{(r)}, \quad \bar{\boldsymbol{\sigma}}_t = \sum_{r=1}^{N} c_r \boldsymbol{\sigma}_t^{(r)}. \tag{41}
$$

Combining (40) and (41) yields the macroscopic constitutive law

$$
\begin{aligned}
\bar{\boldsymbol{\sigma}}_n &= \overline{\boldsymbol{L}}_{nn} \cdot \bar{\boldsymbol{\varepsilon}}_n + \overline{\boldsymbol{L}}_{nt} \cdot \bar{\boldsymbol{\varepsilon}}_t + \bar{\boldsymbol{\sigma}}_n^p, \\
\bar{\boldsymbol{\sigma}}_t &= \left[\overline{\boldsymbol{L}}_{nt} \right]^T \cdot \bar{\boldsymbol{\varepsilon}}_n + \overline{\boldsymbol{L}}_{tt} \cdot \bar{\boldsymbol{\varepsilon}}_t + \bar{\boldsymbol{\sigma}}_t^p,
\end{aligned} \tag{42}
$$

where

$$\begin{aligned}
\overline{\boldsymbol{L}}_{nn} &= \sum_{q=1}^{N} c_q \boldsymbol{L}_{nn}^{(q)} \cdot \boldsymbol{A}_{nn}^{(q)} = \left[\sum_{q=1}^{N} c_q \left[\boldsymbol{L}_{nn}^{(q)} \right]^{-1} \right]^{-1}, \\
\overline{\boldsymbol{L}}_{nt} &= \sum_{q=1}^{N} c_q \left[\boldsymbol{L}_{nn}^{(q)} \cdot \boldsymbol{A}_{nt}^{(q)} + \boldsymbol{L}_{nt}^{(q)} \right] = \overline{\boldsymbol{L}}_{nn} \cdot \left[\sum_{q=1}^{N} c_q \left[\boldsymbol{L}_{nn}^{(q)} \right]^{-1} \cdot \boldsymbol{L}_{nt}^{(q)} \right], \\
\overline{\boldsymbol{L}}_{tt} &= \sum_{q=1}^{N} c_q \left[\left[\boldsymbol{L}_{nt}^{(q)} \right]^{T} \cdot \boldsymbol{A}_{nt}^{(q)} + \boldsymbol{L}_{tt}^{(q)} \right], \\
&= \sum_{q=1}^{N} c_q \left[\left[\boldsymbol{L}_{nt}^{(q)} \right]^{T} \cdot \left[\boldsymbol{L}_{nn}^{(q)} \right]^{-1} \cdot \left[\overline{\boldsymbol{L}}_{nt} - \boldsymbol{L}_{nt}^{(q)} \right] + \boldsymbol{L}_{tt}^{(q)} \right], \qquad (43)
\end{aligned}$$

and

$$\begin{aligned}
\overline{\boldsymbol{\sigma}}_{n}^{p} &= \sum_{r=1}^{N} c_r \boldsymbol{\sigma}_{n}^{p(r)} + \sum_{r=1}^{N} \sum_{q=1}^{N} c_r c_q \boldsymbol{L}_{nn}^{(r)} \cdot \boldsymbol{A}_{nn}^{p(qr)} \cdot \left[\boldsymbol{\sigma}_{n}^{p(q)} - \boldsymbol{\sigma}_{n}^{p(r)} \right] \\
&= \sum_{r=1}^{N} c_r \boldsymbol{\sigma}_{n}^{p(r)} + \sum_{r=1}^{N} \sum_{q=1}^{N} c_r c_q \overline{\boldsymbol{B}}_{nn}^{p(q)} \cdot \left[\boldsymbol{\sigma}_{n}^{p(q)} - \boldsymbol{\sigma}_{n}^{p(r)} \right], \\
\overline{\boldsymbol{\sigma}}_{t}^{p} &= \sum_{r=1}^{N} c_r \boldsymbol{\sigma}_{t}^{p(r)} + \sum_{r=1}^{N} \sum_{q=1}^{N} c_r c_q \left[\boldsymbol{L}_{nt}^{(r)} \right]^{T} \cdot \boldsymbol{A}_{nn}^{p(qr)} \cdot \left[\boldsymbol{\sigma}_{n}^{p(q)} - \boldsymbol{\sigma}_{n}^{p(r)} \right] \\
&= \sum_{r=1}^{N} c_r \boldsymbol{\sigma}_{t}^{p(r)} + \sum_{r=1}^{N} \sum_{q=1}^{N} c_r c_q \overline{\boldsymbol{B}}_{nt}^{p(qr)} \cdot \left[\boldsymbol{\sigma}_{n}^{p(q)} - \boldsymbol{\sigma}_{n}^{p(r)} \right], \\
\overline{\boldsymbol{B}}_{nn}^{p(q)} &= \overline{\boldsymbol{L}}_{nn} \cdot \left[\boldsymbol{L}_{nn}^{(q)} \right]^{-1}, \qquad \overline{\boldsymbol{B}}_{nt}^{p(qr)} = \left[\boldsymbol{L}_{nt}^{(r)} \right]^{T} \cdot \left[\boldsymbol{L}_{nn}^{(r)} \right]^{-1} \cdot \overline{\boldsymbol{B}}_{nn}^{p(q)}. \qquad (44)
\end{aligned}$$

5. Numerical example

Let's consider a periodically multilayered composite structure, whose unit cell consists of two layers with equal volume fraction (50% each). The first layer is an elastic material, while the second is made of an elastoplastic, J_2 type material with isotropic hardening of power law:

$$R(p) = Hp^m. \qquad (45)$$

In the above expression, R is the hardening function, p is the accumulated plastic strain variable and H, m are the hardening parameter and hardening exponent, respectively. The material parameters of the two layers are summarized in Table 1.

parameter	layer 1	layer 2
Young's modulus (MPa)	400000	75000
Poisson's ratio	0.2	0.3
elastic limit (MPa)	–	75
hardening parameter (MPa)	–	416
hardening exponent	–	0.3895

Table 1: Material properties of multilayered composite's layers.

A rectangular structure of dimensions 1 mm$\times$1 mm$\times$0.08 mm is made of the multilayered composite and it is subjected to displacement boundary conditions, which are illustrated in Figure 2. At the boundary surface normal to x_1 direction (positive side), the structure is subjected to a displacement field, which first increases linearly up to 0.002 mm and then decreases linearly until it becomes 0.

The finite element computations have been performed using the FE commercial software ABAQUS/Standard. At the first numerical analysis, no homogenization has been performed. Instead, the structure is simulated considering the different layers. This simulation is the reference solution since it considers all the microstructural details without scale separation. To have a representative structure compatible with the homogenization theory

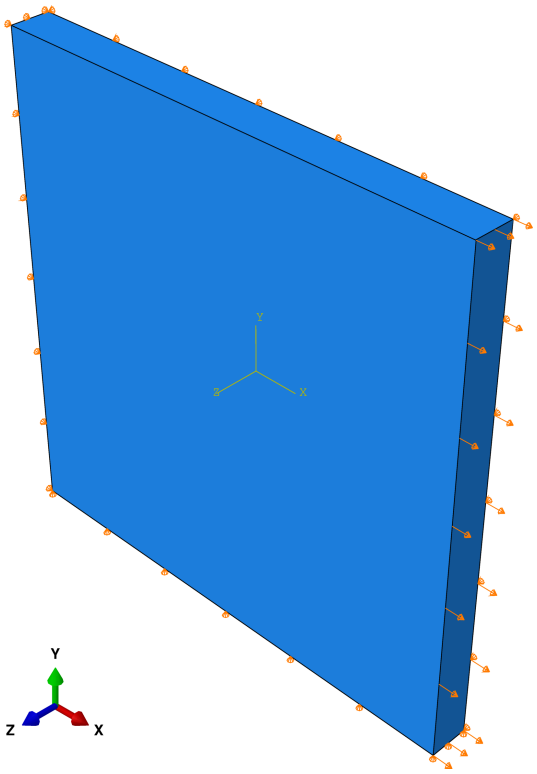

Figure 2: Rectangular structured made of the multilayered composite. The displacement is fixed in three phases (normal to x_1, x_2, x_3, negative sides), two phases (normal to x_2, x_3, positive sides) are traction free and the last phase (normal to x_1, positive side) is subjected to varying displacement field.

(i.e. unit cell much smaller than the macroscopic scale), 50 layers have been considered (25 of each material). The von Mises stress at the end of the loading in shown in Figure 3. As expected, the stress distribution os highly non-uniform due to the strong heterogeneity.

At the second numerical analysis, the Mori-Tanaka/TFA homogenization approach is considered. The equations of section (4) are implemented in

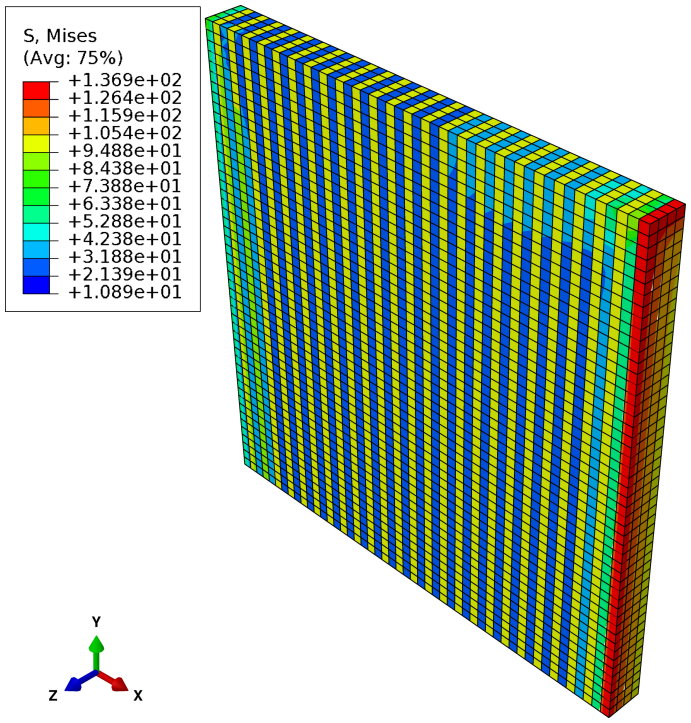

Figure 3: Multilayered composite structure without scale separation. Spatial distribution of von Mises stress at the end of loading.

an incremental, iterative manner. The algorithm for this procedure is given in Figure 4. The internal variables mentioned in the algorithm include the elastoplastic stress tensor $\boldsymbol{\sigma}^{p(2)}$ and the accumulated plastic strain $p^{(2)}$ of the second layer. Each layer has its own constitutive law, which is written as a User Material (UMAT) FORTRAN subroutine. Moreover, the last step of the algorithm requires the computation of a macroscopic tangent modulus. This fourth order tensor for the elastoplastic medium depends on the plastic strain, and it is evaluated from equations (43) by substituting the elasticity tensors with the tangent modulus tensors of the layers. The tangent modulus of an elastoplastic, J_2 type material is discussed frequently in the literature

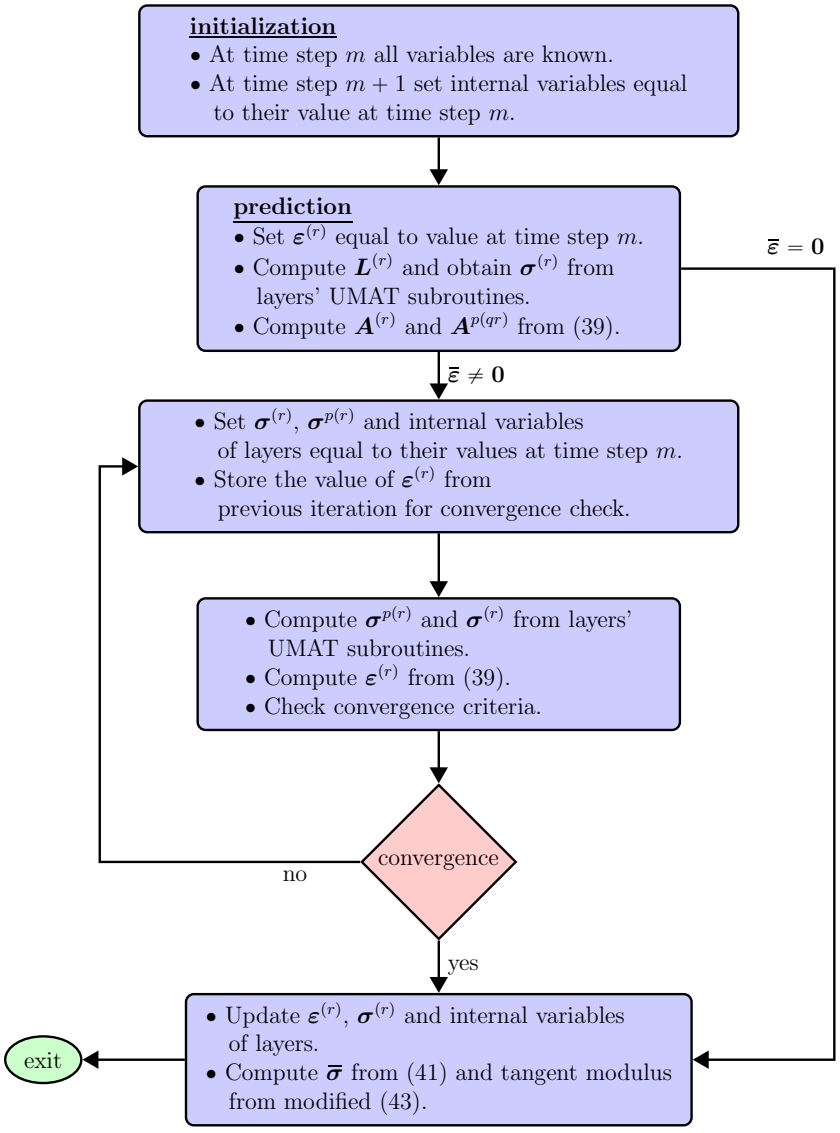

Figure 4: Computational algorithm (Meta-UMAT) for the homogenization of multilayered composites. Mori-Tanaka/TFA approach.

(Simo and Hughes, 1998; Chatzigeorgiou et al., 2018) and is not presented here.

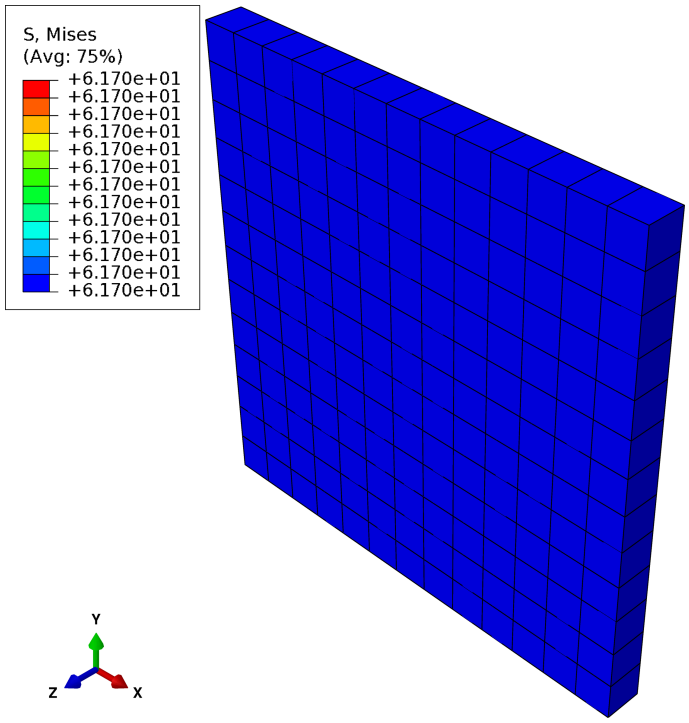

Figure 5: Multilayered composite structure with homogenized response. Spatial distribution of von Mises stress at the end of loading.

The algorithm of Figure 4 is developed in the form of a FORTRAN coded Meta-UMAT and is integrated into the ABAQUS software. Due to the homogenized nature of the medium, the mesh of the structure is not required to be fine. The von Mises stress at the end of the loading in shown in Figure 5. Since there is only one material (the homogenized), the stress is uniform at the whole structure.

Comparison of the macroscopic response (i.e. average stress-strain curve) for the two analyses is given in Figure 6. As it can be seen, the homogenization results are in almost perfect agreement with those of the full structure

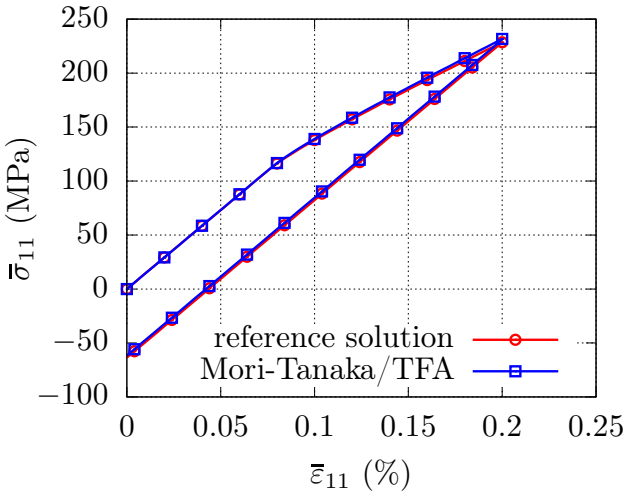

Figure 6: Macroscopic stress 11 vs macroscopic strain 11. Comparison between the layered structure (reference solution) and the homogenization approach.

analysis, validating the accuracy of the mean-field methodology.

As an additional validation of the proposed method, the structure of Figure 3 is analyzed using classical FE type homogenization approach with periodic boundary conditions. The unit cell of Figure 7 represents the periodic microstructure. Due to the simple nature of the loading, one can consider the constraint driver technique (Praud, 2018). In this technique, the macroscopic conditions (given normal macroscopic strain at the direction x_1, zero macroscopic stresses at the rest of normal and shear directions) are applied at ”dummy nodes" which are connected through periodicity conditions with the boundaries of the unit cell.

Figure 8 demonstrates the results obtained from the FE analysis on the unti cell and from the proposed mean-field approach. Both curves are in

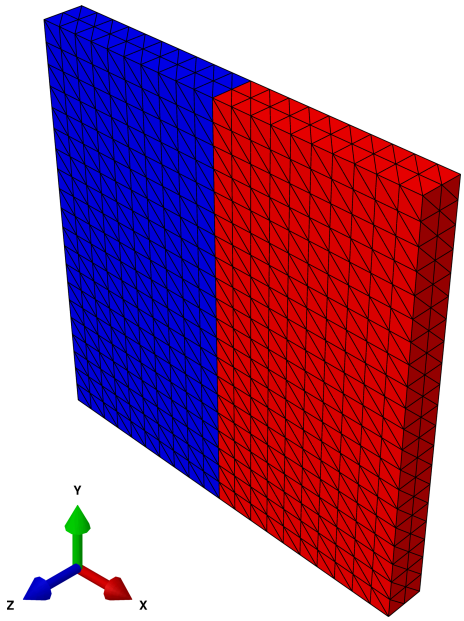

Figure 7: Unit cell of the multilayered composite. Periodicity conditions are applied and the macroscopic loading is imposed through the constraint driver technique. Layer 1 is at the left side and layer 2 at the righr side.

excellent agreement. While the FE type periodic homogenization provides equivalent results with the Mori-Tanaka/TFA method, the latter has the advantage of significantly reduced computational cost. In complex multilayered structures with non-proportional and non-uniform boundary conditions, one has to adopt a FE^2 type of approach (Feyel and Chaboche, 2000), i.e. solving simultaneously FE problems at the structural level and at unit cells corresponding to every macroscopic Gauss point. Such technique is computationally very expensive. Even if the unit cell is described with only one finite element per layer (minimum necessary for correct results), the passage from FE to FE analysis is still time consuming in commercial codes. The proposed method on the other hand is applied in an existing FE code as a

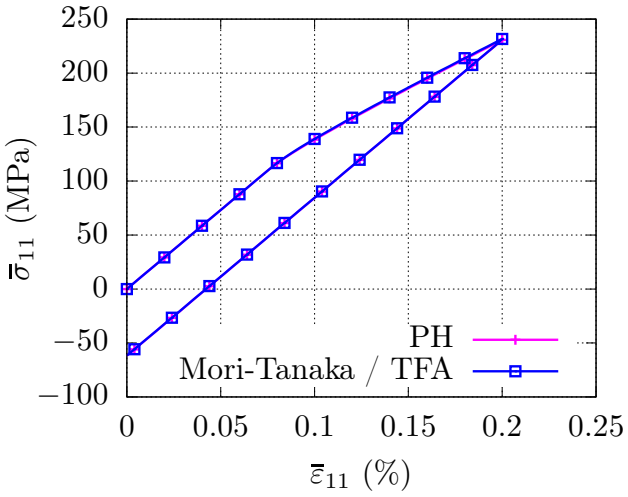

Figure 8: Macroscopic stress 11 vs macroscopic strain 11. Comparison between FE type periodic homogenization (PH) and the proposed method.

standard constitutive law (UMAT in the terminology of ABAQUS), which leads to fast calculations.

6. Conclusions

As it has been demonstrated in this article, the Mori-Tanaka approach combined with the Transformation Field Analysis yields exactly the same solution with the periodic homogenization method for the multilayered composites. These structures are quite simple for performing finite element computations and provide the capability to validate the results of homogenization. Such validation is important when developing micromechanics techniques for complex and/or non-typical material responses, including multiphysics phenomena.

It is worth mentioning that the proposed approach can be applied, under certain conditions, for the study of laminate composites, i.e. layers of long-fiber reinforced media stacked at different orientations. However, one needs to be aware of the method limitations. The multilayered composite presented here is assumed to have theoretically infinite repetitions of unit cells. The main reason for this requirement is that the periodic homogenization methodology considers that the external boundary conditions do not affect the unit cell periodicity conditions. In practice, the method has shown to work relatively well even for moderate number of unit cell repetitions. The laminate composites usually contain a few number of layers, whose stacking sequence is not necessarily periodic. For reduced number of layers, the boundary effects may be very important at the level of the unit cell, leading to wrong homogenization approach predictions. These effects can be accounted for more accurately by higher order homogenization theories, or plate-type homogenization strategies (Kalamkarov and Kolpakov, 1997; Xia et al., 2003) which exceed the capabilities of the classical Mori-Tanaka method.

References

Aboudi, J., 2004. Micromechanics-based thermoviscoelastic constitutive equations for rubber-like matrix composites at finite strains. International Journal of Solids and Structures 41, 5611–5629.

Aboudi, J., Pindera, M.J., Arnold, S.M., 2003. Higher-order theory for periodic multiphase materials with inelastic phases. International Journal of Plasticity 19, 805–847.

Asada, T., Ohno, N., 2007. Fully implicit formulation of elastoplastic homogenization problem for two-scale analysis. International Journal of Solids and Structures 44, 7261–7275.

Barral, M., Chatzigeorgiou, G., Meraghni, F., Léon, R., 2020. Homogenization using modified Mori-Tanaka and TFA framework for elastoplastic-viscoelastic-viscoplastic composites: Theory and numerical validation. International Journal of Plasticity 127, 102632.

Bensoussan, A., Lions, J., Papanicolaou, G., 1978. Asymptotic methods for periodic structures. North Holland, Amsterdam.

Benveniste, Y., 1987. A new approach to the application of Mori-Tanaka's theory in composite materials. Mechanics of Materials 6, 147–157.

Benveniste, Y., Dvorak, G.J., Chen, T., 1991. On diagonal and elastic symmetry of the approximate effective stiffness tensor oh heterogeneous media. Journal of the Mechanics and Physics of Solids 39, 927–946.

Brassart, L., Stainier, L., Doghri, I., Delannay, L., 2012. Homogenization of elasto-(visco) plastic composites based on an incremental variational principle. International Journal of Plasticity 36, 86–112.

Brenner, R., Suquet, P., 2013. Overall response of viscoelastic composites and polycrystals: exact asymptotic relations and approximate estimates. International Journal of Solids and Structures 50, 1824–1838.

Buryachenko, V., 2007. Micromechanics of Heterogeneous Materials. Springer, Berlin.

Cavalcante, M.A.A., Marques, S.P.C., Pindera, M.J., 2009. Transient thermomechanical analysis of a layered cylinder by the parametric finite-volume theory. Journal of Thermal Stresses 32, 112–134.

Cavalcante, M.A.A., Pindera, M.J., 2016. Generalized FVDAM theory for elastic-plastic periodic materials. International Journal of Plasticity 77, 90–117.

Chaboche, J., Kanoute, P., Ross, A., 2005. On the capabilities of mean field approaches for the description of plasticity in metal matrix composites. International Journal of Plasticity 21, 1409–1434.

Charalambakis, N., 2010. Homogenization Techniques and Micromechanics. A Survey and Perspectives. Applied Mechanics Reviews 63, 030803.

Charalambakis, N., Chatzigeorgiou, G., Chemisky, Y., Meraghni, F., 2018. Mathematical homogenization of inelastic dissipative materials: A survey and recent progress. Continuum Mechanics and Thermodynamics 30, 1–51.

Chatzigeorgiou, G., Charalambakis, N., Chemisky, Y., Meraghni, F., 2016. Periodic homogenization for fully coupled thermomechanical modeling of dissipative generalized standard materials. International Journal of Plasticity 81, 18–39.

Chatzigeorgiou, G., Charalambakis, N., Chemisky, Y., Meraghni, F., 2018. Thermomechanical Behavior of Dissipative Composite Materials. ISTE Press - Elsevier, London.

Chatzigeorgiou, G., Chemisky, Y., Meraghni, F., 2015. Computational micro

to macro transitions for shape memory alloy composites using periodic homogenization. Smart Materials and Structures 24, 035009.

Chen, Q., Chatzigeorgiou, G., Meraghni, F., 2021. Extended Mean-Field Homogenization of Viscoelastic-Viscoplastic Polymer Composites Undergoing Hybrid Progressive Degradation Induced by Interface Debonding and Matrix Ductile Damage. International Journal of Solids and Structures 210-211, 1–17.

Desrumaux, F., Meraghni, F., Benzeggagh, M.L., 2001. Generalised Mori-Tanaka Scheme to Model Anisotropic Damage Using Numerical Eshelby Tensor. Journal of Composite Materials 35, 603–624.

Doghri, I., Ouaar, A., 2003. Homogenization of two-phase elasto-plastic composite materials and structures: Study of tangent operators, cyclic plasticity and numerical algorithms. International Journal of Solids and Structures 40, 1681–1712.

Dvorak, G., Benveniste, Y., 1992. On transformation strains and uniform fields in multiphase elastic media. Proceedings of the Royal Society of London A 437, 291–310.

Dvorak, G.J., 2013. Micromechanics of Composite Materials. Springer, Dordrecht.

Feyel, F., Chaboche, J.L., 2000. FE^2 multiscale approach for modelling the elastoviscoplastic behaviour of long fibre SiC/Ti composite materials. Computational Methods in Applied Mechanics and Engineering 183, 309–330.

Fish, J., Chen, W., 2001. Higher-order homogenization of initial/boundary-value problem. Journal of Engineering Mechanics 127, 1223–1230.

Fish, J., Shek, K., Pandheeradi, M., Shephard, M., 1997. Computational plasticity for composite structures based on mathematical homogenization: Theory and practice. Computer Methods in Applied Mechanics and Engineering 148, 53–73.

Herzog, H., Jacquet, E., 2007. From a shape memory alloys model implementation to a composite behavior. Computational Materials Science 39, 365–375.

Jendli, Z., Meraghni, F., Fitoussi, J., Baptist, D., 2009. Multi-scales modelling of dynamic behaviour for discontinuous fibre SMC composites. Composites Science and Technology 69, 97–103.

Kalamkarov, A.L., Kolpakov, A.G., 1997. Analysis, design and optimization of composite structures. Wiley, West Sussex.

Khatam, H., Pindera, M.J., 2010. Plasticity-triggered architectural effects in periodic multilayers with wavy microstructures. International Journal of Plasticity 26, 273–287.

Kruch, S., Chaboche, J.L., 2011. Multi - scale analysis in elasto - viscoplasticity coupled with damage. International Journal of Plasticity 27, 2026–2039.

Lahellec, N., Suquet, P., 2007. On the effective behavior of nonlinear inelastic composites: I. Incremental variational principles. Journal of the Mechanics and Physics of Solids 55, 1932–1963.

Love, B., Batra, R.C., 2006. Determination of effective thermomechanical parameters of a mixture of two elastothermoviscoplastic constituents. International Journal of Plasticity 22, 1026–1061.

Meraghni, F., Desrumaux, F., Benzeggagh, M.L., 2002. Implementation of a constitutive micromechanical model for damage analysis in glass mat reinforced composite structures. Composites Science and Technology 62, 2087–2097.

Mercier, S., Molinari, A., 2009. Homogenization of elastic-viscoplastic heterogeneous materials: Self-consistent and Mori-Tanaka schemes. International Journal of Plasticity 25, 1024–1048.

Mercier, S., Molinari, A., Berbenni, S., Berveiller, M., 2012. Comparison of different homogenization approaches for elastic-viscoplastic materials. Modelling and Simulation in Materials Science and Engineering 20, 024004.

Mori, T., Tanaka, K., 1973. Average stress in matrix and average elastic energy of materials with misfitting inclusions. Acta Metallurgica 21, 571–574.

Mura, T., 1987. Micromechanics of Defects in Solids. Second, Revised ed., Kluwer Academic Publishers, Dordrecht.

Murat, F., Tartar, L., 1997. H-convergence, in Topics in the mathematical modelling of composite materials, in: Cherkaev, A., Kohn, R.V. (Eds.), Progress in Nonlinear Differential Equations and their Applications. Birkhäuser, Boston. volume 31, pp. 21–43.

Otero, J.A., Rodríguez-Ramos, R., Monsivais, G., Pérez-Alvarez, R., 2005. Dynamical behavior of a layered piezocomposite using the asymptotic homogenization method. Mechanics of Materials 37, 33–44.

Pindera, M.J., Khatam, H., Drago, A.S., Bansal, Y., 2009. Micromechanics of spatially uniform heterogeneous media: A critical review and emerging approaches. Composites Part B: Engineering 40, 349–378.

Ponte-Castañeda, P., Willis, J.R., 1995. The effect of spatial distribution on the effective behavior of composite materials and cracked media. Journal of the Mechanics and Physics of Solids 43, 1919–1951.

Ponte-Castañeda, P., 1991. The effective mechanical properties of nonlinear isotropic composites. Journal of the Mechanics and Physics of Solids 39, 45–71.

Praud, F., 2018. Multi-scale modelling of thermoplastic-based woven composites, cyclic and time-dependent behaviour. Ph.D. thesis. Arts et Métiers ParisTech, Metz.

Praud, F., Chatzigeorgiou, G., Meraghni, F., 2021. Fully integrated multiscale modelling of damage and time-dependency in thermoplastic-based woven composites. International Journal of Damage Mechanics 30, 163–195.

Qu, J., Cherkaoui, M., 2006. Fundamentals of Micromechanics of Solids. Wiley, New Jersey.

Sanchez-Palencia, E., 1978. Non-homogeneous media and vibration theory,

in: Lecture Notes in Physics. Springer-Verlag, Berlin. volume 127, pp. 1–398.

Simo, J.C., Hughes, T.J.R., 1998. Computational Inelasticity. Springer-Verlag, New York.

Suquet, P.M., 1987. Elements of homogenization for inelastic solid mechanics, in: Lecture Notes in Physics. Springer, Berlin. volume 272, pp. 193–278.

Terada, K., Kikuchi, N., 2001. A class of general algorithms for multi-scale analyses of heterogeneous media. Computer Methods in Applied Mechanics and Engineering 190, 5427–5464.

Tikarrouchine, E., Praud, F., Chatzigeorgiou, G., Piotrowski, B., Chemisky, Y., Meraghni, F., 2018. Three-dimensional FE^2 method for the simulation of non-linear, rate-dependent response of composite structures. Composite Structures 193, 165–179.

Tu, W., Pindera, M.J., 2014. Cohesive Zone-Based Damage Evolution in Periodic Materials Via Finite-Volume Homogenization. Journal of Applied Mechanics 81, 101005.

Xia, Z., Zhang, Y., Ellyin, F., 2003. A unified periodical boundary conditions for representative volume elements of composites and applications. International Journal of Solids and Structures 40, 1907–1921.

Yu, Q., Fish, J., 2002. Multiscale asymptotic homogenization for multiphysics problems with multiple spatial and temporal scales: a coupled thermo-viscoelastic example problem. International Journal of Solids and Structures 39, 6429–6452.

A. Disk-like inclusion in infinite anisotropic medium

Figure 9 illustrates a disk-like inclusion in infinite medium. The term inclusion refers to a material zone in which a known homogeneous eigenstrain

$$\boldsymbol{\varepsilon}^* = \begin{bmatrix} \varepsilon_{11}^* \\ \varepsilon_{22}^* \\ \varepsilon_{33}^* \\ 2\varepsilon_{12}^* \\ 2\varepsilon_{13}^* \\ 2\varepsilon_{23}^* \end{bmatrix}, \tag{A.1}$$

is imposed. The three-layers structure is made by the same anisotropic material with elasticity tensor $\boldsymbol{L}$. At the far field there is zero stress and strain. This is the typical form of the Eshelby's inclusion problem. The goal is to identify the total strain in the inclusion as a function of $\boldsymbol{\varepsilon}^*$:

$$\varepsilon_{ij} = -P_{ijkl}\sigma_{kl}^*, \qquad \sigma_{ij}^* = -L_{ijkl}\varepsilon_{kl}^*. \tag{A.2}$$

The constitutive law for the middle layer is written

$$\sigma_{ij} = L_{ijkl}\varepsilon_{kl} + \sigma_{ij}^* = L_{ijkl}\frac{\partial u_k}{\partial x_l} + \sigma_{ij}^*. \tag{A.3}$$

Due to the form of the structure, all fields vary spatially only in the x_1 direction, transforming the equilibrium into an 1-D problem. For the simplicity of the subsequent expressions, the elasticity tensor is decomposed with the help of the section 2 representations. Since all fields depend only on x_1, the equilibrium equations are reduced for the middle layer to

$$\frac{\mathrm{d}}{\mathrm{d}x_1}\left(\boldsymbol{L}_{nn}\cdot\frac{\mathrm{d}\boldsymbol{u}}{\mathrm{d}x_1} + \boldsymbol{\sigma}_n^*\right) = \boldsymbol{0}, \tag{A.4}$$

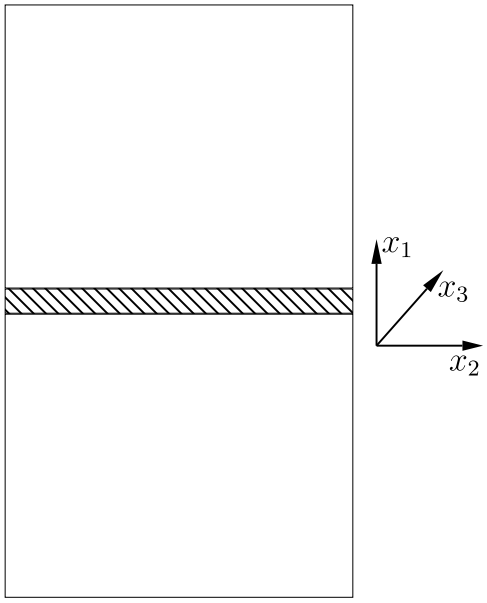

Figure 9: Three-layers structure with small disk-like inclusion at the middle.

with

$$\boldsymbol{u} = \begin{bmatrix} u_1 \\ u_2 \\ u_3 \end{bmatrix}, \qquad \frac{\mathrm{d}\boldsymbol{u}}{\mathrm{d}x_1} = \begin{bmatrix} \varepsilon_{11} \\ 2\varepsilon_{12} \\ 2\varepsilon_{13} \end{bmatrix} = \boldsymbol{\varepsilon}_n. \tag{A.5}$$

For the external layers, where the eigen-strain is zero, the equilibrium yields the trivial solution $\boldsymbol{\sigma}_n = \mathbf{0}$. At the interface between the external and the middle layers the traction is continuous, thus

$$\boldsymbol{L}_{nn} \cdot \boldsymbol{\varepsilon}_n + \boldsymbol{\sigma}_n^* = \mathbf{0}, \tag{A.6}$$

or

$$\boldsymbol{\varepsilon}_n = -\boldsymbol{L}_{nn}^{-1} \cdot \boldsymbol{\sigma}_n^*. \tag{A.7}$$

The tangential strain part, $\boldsymbol{\varepsilon}_t$, is zero. Consequently, the Hill polarization

tensor $\boldsymbol{P}$ can be expressed in the matrix form

$$\boldsymbol{P} = \begin{bmatrix} Z_{11} & 0 & 0 & Z_{12} & Z_{13} & 0 \\ 0 & 0 & 0 & 0 & 0 & 0 \\ 0 & 0 & 0 & 0 & 0 & 0 \\ Z_{21} & 0 & 0 & Z_{22} & Z_{23} & 0 \\ Z_{31} & 0 & 0 & Z_{32} & Z_{33} & 0 \\ 0 & 0 & 0 & 0 & 0 & 0 \end{bmatrix} = \boldsymbol{\mathcal{I}}_n \cdot \boldsymbol{Z} \cdot \boldsymbol{\mathcal{I}}_n^T, \quad \boldsymbol{Z} = \boldsymbol{L}_{nn}^{-1}. \qquad \text{(A.8)}$$